International Journal of Disaster Risk Reduction 72 (2022) 102849

Contents lists available at ScienceDirect

International Journal of Disaster Risk Reduction

journal homepage: www.elsevier.com/locate/ijdrr

Characterizing individual mobility perturbations in cities during extreme weather events

Xinyuan Zhang [a], Nan Li [a,b,*]

[a] Department of Construction Management, Tsinghua University, Beijing, 100084, China
[b] Hang Lung Center for Real Estate, Tsinghua University, Beijing, 100084, China

ARTICLE INFO

Keywords:
Individual mobility pattern
Mobility perturbation
Individual variation
Extreme weather event

ABSTRACT

Understanding the patterns of urban human mobility has played an important role in multiple disciplines such as urban planning, transportation engineering and social sciences. Due to its rich connotations related to urban regions, the extreme weather events (EWEs)-induced perturbation of human mobility has been studied to capture the multifaceted influences of EWEs on cities. While this issue has drawn increasing attention, there is still limited understanding of EWE-induced mobility perturbation at the individual level. To address this need, a new analytical framework for individual mobility perturbation is proposed in this study. The framework assesses individual mobility perturbation during EWEs by taking various facets of spatial and temporal features into consideration, and examines the individual variation of such perturbation. To demonstrate the efficiency of the proposed framework, two consecutive typhoon events that influenced the city of Guangzhou, China in summer 2017 were examined as a case study. It was found that individuals in the city experienced notable decreases in the number of visited locations, visitation frequency and movement range, increases in waiting time, and changes in movement status pattern under these two EWEs. Moreover, mobility perturbation showed significant variation among individuals, and such variation was linked to individuals' demographic attributes, home location and travel preference. Meanwhile, four types of responses to EWE impacts were extracted from the population. The findings in this study contribute to a manifold understanding of EWE-induced individual mobility perturbations, and have potential to be transformed into actionable measures in urban EWE risk reduction and management practices.

1. Introduction

The world has witnessed increasing frequency and intensity of extreme weather events (EWEs) in the past decades [1,2], which have imposed significant threats to cities worldwide. This has inspired an increasing amount of researches on assessing EWE-induced impacts on cities, in terms of e.g. building and infrastructure damages [3], economic losses [4] and community disruptions [5], and developing solutions to enhance cities' adaptation and resilience [6,7]. More recently, urban human mobility has provided a new insight to study EWE-induced impacts on cities. Urban human mobility is the interactions between individuals and physical settings in the city [8]. Urban form [9], transportation infrastructure [10] and the distribution of hotspots in the city [11] shape urban human mobility. Meanwhile, mobility is also the way individuals access various resources and opportunities in the city [12]. The job opportunities and jobs-housing relationship determine people's commuting behavior and the travel flow of residents in the city [13,14].

* Corresponding author.
E-mail address: nanli@tsinghua.edu.cn (N. Li).

https://doi.org/10.1016/j.ijdrr.2022.102849
Received 30 June 2021; Received in revised form 15 December 2021; Accepted 11 February 2022
Available online 16 February 2022

According to this view, human mobility perturbation, which is considered as the disturbed spatial-temporal characteristics in human mobility [15–17], has been regarded as an indicator to extract and understand the failure of urban infrastructure system, the anomaly of socio-economic activities and the change of people's behavioral patterns under EWEs. Therefore, researchers have looked into the EWE-induced human mobility perturbation in urban regions to capture the multifaceted influences of EWEs in urban regions.

Prior studies that investigated human mobility perturbations caused by EWEs or other types of extreme events mostly focused on perturbations at the population level. A number of metrics, such as total displacement [15], population transitions [18], relative total distance and accumulated perturbation [16], were introduced in prior research to quantify and analyze the overall mobility perturbation in a region. Different from mobility perturbation at the population level, individual mobility perturbation refers to the disturbed spatial-temporal characteristics of each individual's mobility during EWEs, which reflects the changes in individual's travel intention, travel preference and mobility pattern. Uncovering mobility perturbation at the individual level helps with demonstrating how individuals react and change their travel behaviors under the impact of EWEs, which in turn explains the perturbations of aggravated mobility. Besides, while making evacuation plans, pre-EWE preparations and crisis response strategies, city managers sometimes concern special groups, e.g. vulnerable individuals and people living within evacuation zones, rather than the entire population. Analyses of individual mobility perturbation contribute to identifying vulnerable individuals and exploring individual variations of mobility perturbation. Despite its critical roles, existing understanding of individual mobility perturbation is still limited.

More specifically, the above gap is twofold. First, while a few studies have attempted to assess individual mobility perturbations [15,19,20], they mainly relied on qualitative analysis and only considered limited characteristics of individual mobility. However, human mobility is characterized with various spatial and temporal features, such as visited locations, movement range, waiting time and movement status, whose patterns cannot be integrally described by a single indicator. This calls for consideration of various facets of mobility characteristics when quantifying individual mobility perturbation, which has largely remained underexplored in the existing literature. Further adding to the need of considering multiple characteristics in the analysis of individual mobility perturbation is the fact that it would provide a chance for cross-validation between different patterns, which is important for providing a manifold understanding of people's reactions to EWEs and supporting accurate prediction of people's movement under the influence of EWEs.

Second, prior studies have found that the influence of EWEs on human mobility is highly diverse among individuals [21], and that various factors, such as gender, financial situation and normal mobility pattern, may have contributed to such diversity [20,22]. However, the individual variation of mobility perturbation has largely remained to be explored. By studying the correlations between individuals' characteristics and their mobility perturbations, the underlying factors that influence individual mobility perturbation during EWEs could be revealed. These key factors might help answer why people's mobility patterns change during EWEs and what cause the variation in individual mobility perturbation, which would have significant implications for urban disaster risk reduction practices that involve e.g. traffic management and emergency response resources allocation.

To address the above knowledge gap, this study aims to propose an analytical framework for quantifying individual mobility perturbation with various spatial and temporal features and investigating the individual variation of such perturbation. This framework consists of three modules. First, a series of metrics are introduced for characterizing individual mobility patterns in terms of visited locations, movement range, waiting time and movement status. Then, based on these metrics, the framework incorporates methods for analyzing, both qualitatively and quantitatively, whether and to what extent individual mobility patterns are affected by EWEs. Finally, the framework addresses the key factors accounting for individual variations of mobility perturbation, by examining the correlations between individuals' characteristics and their mobility perturbations. Then, individuals are clustered into several groups based on their different types of responses to EWEs in terms of the mobility perturbation. Typhoon Hato and Typoon Pakhar, two consecutive EWEs that influenced the city of Guangzhou, China in a single week, are examined as a case study. The findings in this study are expected to contribute to the existing body of knowledge about EWE-induced mobility perturbation, and provide city managers with new insights that would allow them to make more informed decisions for enhanced resilience of cities against EWEs impact.

2. Literature review

2.1. Metrics for characterizing individual mobility patterns

The mobility trajectories of an individual, which can be described as a time-stamped consecutive sequence of locations the individual visits [23], have a high degree of spatial and temporal regularity [24,25]. This suggests that, to comprehensively characterize individual mobility patterns, both spatial and temporal characteristics should be considered.

Accordingly, a variety of metrics have been introduced in prior research to describe the spatial and temporal characteristics of human mobility. Among those that focus on individual mobility patterns, the metrics of travel length and waiting time [26] are the most fundamental ones. Providing basic information about every trip made by an individual, these two metrics form the cornerstone of early models of individual mobility, such as the well-known continuous time random walks (CTRW) model [27]. Beyond separated trips, prior research also investigated the characteristics of individuals' trajectories that comprise a sequence of trips, for which a few metrics, such as the number of visited locations and visitation frequency [28], were introduced. In addition, the spatial distribution of visited locations is also important, especially for understanding the diffusive process of individual mobility. To quantify this characteristic, González et al. adopted a time-independent characteristic travel distance termed radius of gyration to describe the individual movement range [24]. Furthermore, individuals were found to have a tendency of returning to a few frequently visited locations [24,29], which has motivated a few metrics that are used to describe individuals' recurrent mobility pattern and its impact on individuals' overall mobility patterns. These metrics include: (1) k-radius of gyration (the radius of gyration computed over top k most frequently visited locations) [29], (2) k-visitation frequency (visitation frequency to the kth most frequently visited locations) [30], (3)

k-waiting time (waiting time in the kth most frequently visited locations) [31], and (4) return time (inter-event time between two consecutive visits to the same visited location) [32]. More recently, with the increasing use of complex network approaches in urban mobility analysis, network-based metrics, such as average degree and average path length [33], have also been introduced to assess the topological characteristics of mobility networks that are extracted from individuals' trajectories.

2.2. Influence of EWEs on urban human mobility

Prior studies have reported that EWEs would cause short-term perturbations to urban mobility and, in extreme cases, lead to long-term immigration [16,22]. A number of studies have investigated the influences of EWEs on urban mobility at the population level and revealed that the intensity of human mobility and the travel flow of urban population perturbed during EWEs [16,34].

Meanwhile, there is relatively a scarcity of research that assessed the mobility perturbation at the individual level. Among the few researchers that have looked into this problem, Wang et al. discovered that the statistical properties of individuals' radius of gyration would be notably perturbed under the influence of severe winter storms [19]. They also found that, affected by Hurricane Sandy, the number of long-distance trips by people in New York City decreased while the number of short-distance trips increased [15]. In another study, the impact of EWEs on individual human mobility was assessed based on the shifting distance of the center of mass of individuals' trajectories [20]. In addition, although individual mobility tends to have a high degree of regularity characterized by a few highly frequented locations [24,29], such regularity was found to be weaker during EWEs [19]. Findings in the above studies proved the significance of individual mobility perturbation during EWEs. However, these analyses and findings were mainly qualitative, and there still lacks an effective approach for assessing the magnitude of such perturbation. Moreover, prior studies examined individual mobility perturbation only through changes in travel length, radius of gyration and center of mass, while other important characteristics, such as the number of visited locations, visitation frequency, waiting time and movement status, were largely neglected.

Another important knowledge gap in literature is related to the understanding of key factors influencing EWE-induced individual mobility perturbation. The individual mobility perturbation is highly diverse among different individuals [20,22,33]. Yet, the underlying reasons for such diversity have remained underexplored. According to prior studies, the diversity of individual mobility perturbation could be possibly attributed to the following factors. First, demographic attributes, such as age, gender, occupation, race and class, are believed to have impact on people's reactions to changing environment as well as their mobility perturbations [35,36]. For instance, it was discovered that long-term immigration caused by flooding and crop failures was visibly more intense for women and the poor [22]. Second, it has been discovered that home location, which represents one's primary habitat [37], correlates with mobility patterns. The variations of population density, infrastructure development, job opportunity and land use around people's primary habitats result in the diversity of individual mobility patterns [38]. Besides, the intensity of EWE-induced impact and its recovery also differ across regions in a city [39]. Therefore, during EWEs, people who live in different places will be affected by the EWE-induced infrastructure failure and service disruptions differently [40,41], which likely contributes to the individual variation of mobility perturbation. Third, people's mobility perturbation is correlated with their mobility pattern in steady states. For instance, Wang et al. noticed that individuals with more recurrent locations showed a higher correlation between recurrent mobility and perturbed mobility [19], which suggested that their mobility patterns during abnormal times were more predictable. In addition, the

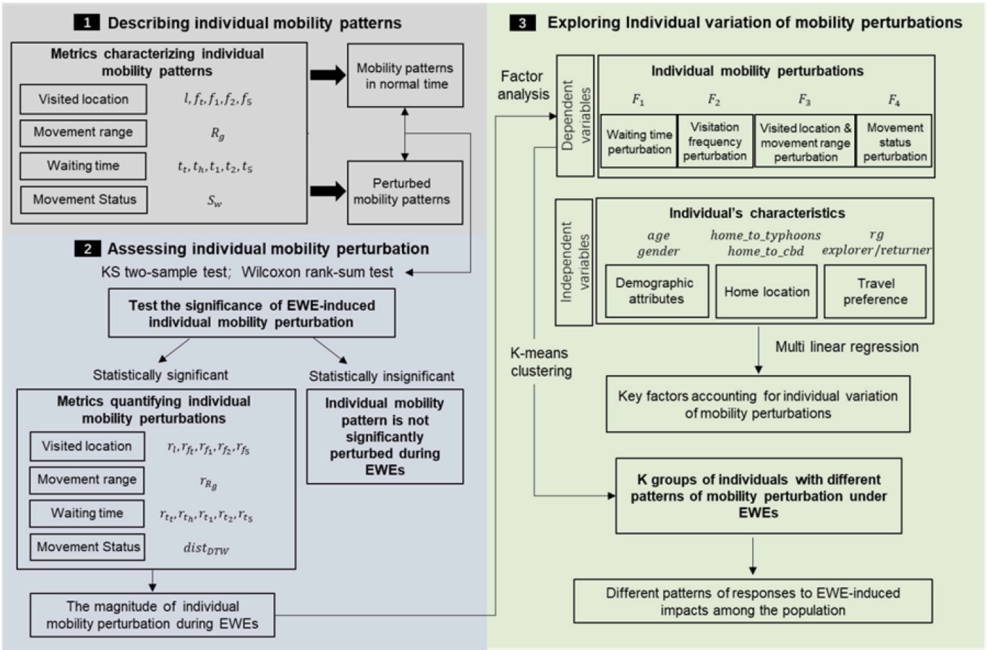

Fig. 1. The analytical framework for individual mobility perturbation.

shifting distance of center of mass was also found to be positively correlated with the radius of gyration in steady states [20]. Despite the above sporadic studies, the individual variation of mobility perturbation has largely remained to be explored.

In summary, a line of researches have confirmed the impact of EWEs on individual mobility and have qualitatively described individual mobility perturbation in terms of travel length, center of mass and regularity. Besides, researchers have also pointed out the individual variation of mobility perturbation and put forward a series of impact factors of individual mobility perturbation. Based on the existing literature, this study aims to develop an effective framework for quantitatively assessing the magnitude of individual mobility perturbation from a more comprehensive perspective that takes a wide range of spatial-temporal characteristics, e.g., the number of visited locations, visitation frequency, waiting time and movement status, into consideration. The framework proposed in this study is expected to replenish the currently limited understanding of the impact of EWEs on individual mobility patterns and its implications for EWE-induced impact assessment and urban resilience enhancement. Moreover, this study also aims to address the individual variation of EWE-induced mobility perturbation. On the one hand, this study identified impact factors of individual mobility perturbation and analyze the correlation between individuals' characteristics and their mobility perturbations, which would explain why people's mobility patterns change during EWEs and identify the main causes of the variation in individual mobility perturbation. On the other hand, this study clustered individuals into groups according to their mobility perturbation. By doing so, several groups of individuals with different responses to EWEs were finally extracted, which contributed to better understanding about the variation of individual mobility perturbation.

3. Analytical framework for individual mobility perturbation

In order to characterize EWE-induced individual mobility perturbation, an analytical framework is proposed in this study. It consists of three modules, as illustrated in Fig. 1. In the first module, a number of metrics are selected to describe individual mobility patterns from various aspects including visited locations, movement range, waiting time and movement status. For the second module, a series of metrics are developed to quantify and analyze individual mobility perturbation under EWEs. Lastly, this framework focuses on exploring the individual variation of mobility perturbations. Key factors contributing to individual variation of mobility perturbations are identified by incorporating methods for analyzing the correlations between individuals' characteristics, described by their demographic attributes, home location and travel preference, and their mobility perturbations. Then, the k-means clustering algorithm is adopted to cluster individuals into several groups based on their mobility perturbations. Each group corresponds to a different pattern of responses to the impact of EWEs. Details of the proposed framework are further explained in the remainder of this section.

3.1. Characterizing individual mobility patterns

As aforementioned, individual mobility trajectories possess a high degree of temporal and spatial regularity [24,25]. Therefore, to characterize individual mobility patterns integrally, both spatial and temporal characteristics are considered in this study.

The spatial characteristics of individual mobility can be reflected by the number, visitation frequency and spatial distribution of visited locations. Accordingly, the following metrics are selected: (1) the number of visited locations (l) and the visitation frequency of all visited locations (f_t) [28] are used to characterize the overall spatial mobility pattern; (2) the visitation frequencies of the top 1, top 2 and top 5 most frequently visited locations (f_1, f_2 *and* f_5) are used to characterize the recurrent spatial mobility pattern [30]; and (3) the radius of gyration (Rg) is used to quantify the movement range, which describes the spatial distribution of visited locations [24]. Rg can be calculated based on Eqs. (1) and (2):

$$R_g = \sqrt{\frac{1}{f_t}\sum_{i=1}^{l} n_i (r_i - r_c)^2} \tag{1}$$

$$r_c = \frac{1}{f_t}\sum_{i=1}^{l} n_i * r_i \tag{2}$$

where f_t is the visitation frequency of all visited locations, n_i is the visitation frequency of visited location i, r_i is the position vector of visited location i, and r_c is the center of mass of mobility trajectory.

On the other hand, the temporal characteristics of individual mobility can be reflected by the allocation of waiting time among all visited locations as well as the travel schedule. The former one characterizes how many times an individual visits each place and how long he/she stays there, while the latter characterizes when an individual tends to stay at each place or move between places. Accordingly, the following metrics are selected: (1) the total waiting time (t_t) is used to characterize the overall temporal mobility pattern [26,31]; (2) the waiting time at home and at the top 1, top 2 and top 5 most frequently visited locations (t_h, t_1, t_2 *and* t_5) is used to characterize the recurrent temporal mobility pattern [31,42]; and (3) a new metric (S_T) is introduced to describe one's daily movement status in the time period T. Specifically, one's movement status throughout *day i* can be characterized by a time series S_i, which can be calculated based on Eq. (3):

$$S_i = \left[s_{i,0}, s_{i,1}, \ldots, s_{i,n}, \ldots, s_{i,47}\right],\ s_{i,n} = 0 \text{ or } 1 \tag{3}$$

where $s_{i,n}$ stands for one's movement status in the *n-th* half hour in *day i.* is a binary variable, with value 0 representing static status, indicating the individual spends majority of this half hour staying at certain locations, and value 1 representing movement status, indicating otherwise.

Based on S_i , one's daily movement status over time period T with a duration of k days, denoted asS_T, can be calculated based on Eq. (4) and Eq. (5):

$$S_T = \left[s_{T,0}, s_{T,1}, \ldots, s_{T,n}, \ldots, s_{T,47}\right] \tag{4}$$

where $s_{T,n}$ denotes the one's daily movement status in the *n-th* half hour over time period T:

$$s_{T,n} = \left(s_{1,\ n} + s_{2,n} + \ldots + s_{k,n}\right)/k \tag{5}$$

In summary, a total of 12 metrics are selected to describe individual mobility patterns in terms of visited locations, movement range, waiting time and movement status. These metrics are summarized in Table 1.

3.2. Assessing individual mobility perturbations

For metrics in Table 1, the average value of each metric in EWE-free days can be calculated to represent individual mobility patterns in normal state, while that in EWE-influenced days reflects perturbed individual mobility patterns. Therefore, for each metric, by comparing its distribution and mean value among all individuals between normal state and perturbed state, whether the individual mobility pattern as reflected by this metric is perturbed during EWE can be determined. For this purpose, specifically, the Kolmogorov-Smirnov (KS) two-sample test [43] can be conducted to examine whether the distribution of each metric during EWE differs from that in normal time, and the Wilcoxon rank-sum test [44] can be conducted to examine whether the mean value of each metric changes during EWE.

If individual mobility perturbations are found to be statistically significant, a series of metrics are developed in the proposed framework for quantifying the magnitude of the perturbations. The change rates of all metrics introduced in Table 1, except metric S_T, can be calculated to quantify the perturbation in visited locations, movement range and waiting time. Specifically, for any metric M, its change rate r_M is calculated based on the following equation:

$$r_M = \frac{M_{EWE} - M_{normal}}{M_{EWE} + M_{normal}} \times 100\% \tag{6}$$

where M_{EWE} represents the value of metric M during EWEs and M_{normal} represents the value of metric M in normal time. This change rate ranges from −100% to 100%, and a negative value represents a decrease of the metric during EWEs.

As for metric S_T, the dynamic time warping (DTW) algorithm [45] is applied to quantify the similarity between S_T values in normal time (S_{normal}) and during EWE (S_{EWE}) based on Eq. (7). DTW algorithm was initially proposed to find an optimal match between two given time series with a high tolerance of outliers [45,46]. According to DTW algorithm, to compare S_{EWE} with S_{normal}, the first step is to construct a 48*48 DTW grid. The value of each grid cell represents the distance between corresponding elements in the two time series (here the absolute value of difference between corresponding elements is used). The next step is to find a path through the grid which minimizes the total distance. The minimized total distance is called the DTW distance between S_{normal} and S_{EWE}, which is denoted as $DTW(S_{EWE}, S_{normal})$. The $DTW(S_{EWE}, S_{normal})$ value is further divided by 48 for normalization purpose, and the resulting variable $dist_{DTW}$ has a value that ranges from 0 to 1:

$$dist_{DTW} = \frac{DTW(S_{EWE}, S_{normal})}{48} \tag{7}$$

where $dist_{DTW}$ measures the perturbation of one's movement status, and a larger value of $dist_{DTW}$ indicates a greater perturbation in

Table 1
Metrics used to characterize individual mobility pattern.

	Metrics	Definition
Visited Location	L	The number of visited locations
	f_t	The visitation frequency to all locations
	f_1	The visitation frequency to the most frequently visited location
	f_2	The visitation frequency to the two most frequently visited locations
	f_5	The visitation frequency to the five most frequently visited locations
Movement Range	R_g	The weighted average distance of all visiting locations to mobility center
Waiting Time	t_t	The waiting time in all locations
	t_h	The waiting time at home
	t_1	The waiting time in the most frequently visited location
	t_2	The waiting time in the two most frequently visited locations
	t_5	The waiting time in the five most frequently visited locations
Movement Status	S_T	The daily movement status during time period T

movement status.

3.3. Analyzing individual variation of mobility perturbations

3.3.1. Individual characteristics

In this proposed framework, individual characteristics are represented by demographic attributes, home location and travel preference, which are considered as three main factors influencing EWE-induced individual mobility perturbation in prior research. To measure these factors, the following variables are selected: (1) for demographic attributes, individuals can be classified based on gender and age group; (2) with respect to home location, it can be measured by two variables, namely the distance between one's home location and the central business district (CBD) of the city (*distance_to_cbd*), and the distance between the home location and the tracks of typhoon (*distance_to_typhoon*). *distance_to_cbd* reflects the variation of population density and infrastructure services in different regions in a city, and *distance_to_typhoon* reflects the variation of impact intensity of typhoon events; (3) as for travel preference, it can be measured by people's preference to return to places they have visited before [29] and their preference to visit distant places. Specifically, it is discovered that people with different preferences to return already-visited places possess highly different mobility patterns. Based on such preference differences, people can be divided into explorers and returners [29,47]. Following the classification method introduced by Pappalardo et al. [29], the ratio of Rg^2 (Eq. (8) and (9)) to Rg (Eq. (1)), denoted as s_2, can be calculated for each individual. Those with s_2 larger than 0.5 are classified as returners or otherwise as explorers. Meanwhile, weekly radius of gyration (Rg) in normal time, which describes individuals' movement range, can be used to assess their preference for distant places.

$$R_g^2 = \sqrt{\frac{1}{f_2}\sum_{i=1}^{2} f_i\left(r_i - r_c^2\right)^2} \tag{8}$$

$$r_c^2 = \frac{1}{f_2}\sum_{i=1}^{2} f_i * r_i \tag{9}$$

3.3.2. Relationship between individual's characteristics and mobility perturbation

The proposed analytical framework uses the multiple linear regression [48], a widely used statistical modeling method, to study the relationship between people's characteristics and their mobility perturbations. In the regression model, categorical variables and numerical variables that describe people's characteristics are treated as independent variables, and the metrics introduced in Section 3.2 that quantify individual mobility perturbations are treated as dependent variables. As such, there are a total of 12 dependent variables in the model. If there are strong correlations between some of the dependent variables, factor analysis, which is a commonly adopted method for reducing the number of variables into fewer independent latent variables [49], should be conducted. To analyze the correlation between these variables and test whether factor analysis should be used, the Kaiser-Meyer-Olkin measure [50] and Bartlett's sphericity test [51] can be conducted on the 12 dependent variables.

3.3.3. Clustering individuals with different responses to EWEs

K-means clustering algorithm, a classic unsupervised learning method, is adopted to cluster individuals into groups with different responses to EWEs [52]. K-means cluster algorithm aims to find the cluster centers such that the sum of squared distance, defined as distortion, of each data point to its nearest cluster center is minimized. The distortion could be calculated based on Eq. (10):

$$distortion = \sum_{i=1}^{n}\left[\underbrace{min}_{k=1,2,\ldots,K} d(x_i, c_k)\right] \tag{10}$$

where K is the number of clusters, c_k is the center of cluster k, d represents the distance function which is chosen as the Euclidean distance in this study.

Here, individuals are clustered based on their mobility perturbation, which is characterized by a multidimensional variable (namely x_i in Eq. (10)) composed of the factors extracted in Section 3.3.2. The approach known as the "Elbow method" is adopted to determine the number of clusters k [53]. Specifically, k-means clustering method is run for k from 1 to 10 and then the value of distortion could be computed for each value of k. According to the Elbow method, the proper number of clusters could be determined based on the relationship between distortion and the number of clusters. Given the chosen k, individuals could be clustered into k groups with different characteristics of individual mobility perturbation accordingly.

4. Case and data

The proposed framework is demonstrated using a case study. The background of the case and details of the studied mobility data are explained in this section. The results of the case study are presented and discussed in the following sections.

4.1. Data descriptions

This work studied individual mobility perturbation in Guangzhou, China, under the impact of two consecutive typhoon events in summer 2017. Guangzhou is a highly-developed subtropical coastal city with dense population and suffers from typhoons and hurricanes at a high frequency every year. Considering its urban form as well as its urban development and management levels, Guangzhou is one of the most representative coastal cities in southern China. Moreover, the studied case is of notable

representativeness for other highly-developed cities around the world that have dense urban population and are faced with similar typhoon or hurricane challenges. The findings of this work have guiding significance to these cities on enhancing urban resilience against EWEs impact.

Guangzhou was severely impacted by two consecutive typhoon events, namely Typhoon Hato and Typhoon Pakhar, in summer 2017. Specifically, Typhoon Hato, a maximum category 16 storm according to China Meteorological Administration tropical cyclone database [54], made a landfall in a neighboring city of Zhuhai on August 23, 2017 and hit Guangzhou in the afternoon. It was the strongest typhoon that impacted Guangzhou in 2017, triggering an orange typhoon alert by China Meteorological Administration the day before the landfall. Four days later, Typhoon Pakhar, a maximum category 10 storm according to China Meteorological Administration tropical cyclone database [54], retraced Typhoon Hato's path and hit Guangzhou again, when the city was still recovering from Typhoon Hato's devastation. These two EWEs influenced Guangzhou for around five consecutive days, causing severe fluvial flooding, pluvial flooding and blackouts, evacuation of over 14 thousand people, widespread delays or cancellations of buses, trains and flights, and citywide closures of businesses, schools and other public facilities [55,56].

The mobility dataset used in this study was anonymized mobile phone geolocation records collected by a Chinese smartphone push-notifications service provider. The company operates a built-in software development kit (SDK) used by a wide range of popular smartphone applications in China to collect geolocation records from mobile phone users who have signed licensing agreements and agreed with the terms of privacy policy. The geolocation records are reported by GPS sensors embedded in mobile devices. The location reporting of the push-notifications service has triggering events, such as location movement, network connections and so on. The studied dataset, which we obtained from the above company under a non-disclosure agreement (NDA), contained geolocation records of 118,619 anonymized individuals over a study period between August 1 and September 30, 2017. Each individual was assigned a unique hashed ID, which could not be used to trace to any specific mobile phone device or person but would allow us to track and analyze the trajectories of each individual over the entire study period. In addition, the study only uncovered empirical findings in an aggregated manner. The above conditions ensured the legality of the mobility dataset and the protection of privacy. Table 2 shows a few sample data entries.

Considering that people's mobility patterns exhibit weekly regularity and that the influence of the two typhoon events lasted from Wednesday, August 23 to Sunday, August 27, only geolocations from Wednesday to Sunday in each weak were used for analyzing individual mobility patterns, and geolocations on Mondays and Tuesdays were excluded during data preprocessing. As such, the final dataset was composed of trajectories over a total of 40 days, in which the geolocations recorded on August 23–27 were used to capture individual mobility patterns perturbed by typhoons and those recorded in other weeks were used to capture individual mobility patterns under normal conditions.

Furthermore, to ensure sufficient and representative geolocation records for capturing the mobility patterns of each individual, only individuals whose trajectories met the following criteria were included in the final dataset: (1) all trajectories of the individual should be located within Guangzhou during the study period; (2) the individual's home location should be identifiable using the following algorithm [38]: the visited location where the individual stays for the longest time between 0 a.m. and 6 a.m. over the study period and for a minimum average of 3 h a day can be identified as this individual's home location; (3) for any given day, the geolocations should be distributed among at least five different hours, otherwise trajectories in this day should be excluded; (4) the individual's trajectories should cover the influence period of the two EWEs, namely August 23–27, 2017; (5) the individual's trajectories should cover at least five entire typhoon-free weeks (from Wednesday to Sunday) during the study period.

After filtering the data with the above criteria, the final dataset used in the following analyses included a total of 53,769 anonymized individuals, which represented a sampling rate of approximately 0.29% of the city's 18.7 million resident population. The spatial resolution for the dataset was approximately 20 m, and the average temporal resolution was approximately 7 min. On average, each individual in the dataset had around 125 timestamped geolocations per day.

As shown in Table 2, the studied dataset also included certain demographic information about the anonymized individuals, including their gender and age group. Specifically, each individual was identified as either male or female, and was categorized in one of the following four age groups, namely 18–24, 25–34, 35–44, and above 45. Individuals under 18 years old were not included in the dataset. The above demographic information was estimated based on the individuals' usage patterns of smartphone applications (APPs) and histories of points of interest (POIs) visitations, using proprietary, non-disclosed algorithms developed by the original source and owner of the studied dataset.

Like datasets used in other urban mobility studies, our dataset was not perfect; rather, it bore two inherent limitations that should be acknowledged. First, given the nature of the dataset, the sampling of the city's population was not entirely random, and was impacted by individuals' accessibility to mobile devices and whether collection of location information was allowed on the mobile

Table 2
Examples of GPS trajectory data entries.

User ID	Timestamp	Longitude	Latitude	Gender	Age group
***73f5	170810004149	113.148	23.465	Female	18–24
***80b9	170801165546	113.838	23.172	Female	35–44
***ea46	170801001508	113.321	23.024	Male	25–34
***73a3	170807213752	113.383	23.126	Female	35–44
***a30b	170801124858	113.308	23.081	Female	18–24
***c1ae	170809131232	113.331	23.023	Female	45+
***1e21	170801223442	113.499	23.472	Male	25–34

devices. Second, the proprietary algorithm adopted to estimate the demographic information had an approximate accuracy of 80% according to the data provider/algorithm developer, which indicated that the influence of estimation errors was likely limited but could not be completely ruled out. To address the above limitations, additional tests were conducted in this study that aimed to assess the representativeness and reliability of the studied dataset. Specifically, based on the estimated home location of every individual in the studied dataset, the spatial distribution of the home locations of all individuals among the 11 districts in Guangzhou was calculated. This distribution was compared to the actual district-level spatial distribution of the city's population according to the latest official census data [57]. The result is illustrated in Fig. 2. Similarly, the gender and age group distributions of all individuals in the studied dataset were compared to the actual gender and age group distributions of the city's population. The result is illustrated in Fig. 3. These two figures showed that the studied dataset generally matched the census data well, except that the proportion of males and the proportion of individuals in age group of 25–34 were slightly larger in the dataset, which probably resulted from a systematic bias of the user group of the data provider.

4.2. Data processing

The geolocations in the studied dataset were processed before analyses. Details of the processing steps are explained as follows.

4.2.1. Detecting mobility phases

To extract mobility patterns from trajectory data, it is important to first identify the places that people actually visit and distinguish them from the places they pass by. There are two separate phases of human mobility, namely the static phase where an individual spends some time in a place, and the moving phase where an individual moves towards a place. A simple heuristic widely used in prior studies was adopted for detecting the two phases: if two consecutive geolocations in an individual's GPS trace p_i and p_{i+1} satisfy inequality (11) [58,59]:

$$\frac{||p_i - p_{i+1}||}{t_{i+1} - t_i} \leq \Delta \tag{11}$$

where t_{i+1} and t_i are the timestamps of p_{i+1} and p_i, respectively, then p_i is considered to belong to the static phase. Since observed human walking speed is generally at 4–5 km/h (1.1–1.4 m/s), the value of Δ in the above inequality is set as 1.3 m/s in consistence with prior studies [59].

4.2.2. Extracting visited locations

After the static phases were identified, the next step of the data processing was to extract visited locations from the static phases. A visited location is defined as a spot where an individual stands still or moves around very slowly for some time [59]. A visitation starts with the individual's arrival at a visited location and ends at the departure. The movement from one visited location to another is defined as a trip. To extract visited locations, the following methods were adopted in this study.

First, based on geolocations belonging to static phases, geolocation clusters were extracted using the DBSCAN (Density-Based Spatial Clustering of Application with Noise) algorithm [60]. This algorithm is widely used in prior studies to remove abnormal geolocation records, and extract the spots that each individual visits from the individual's trajectories [61,62]. As two key DBSCAN parameters, the maximum search radius and the minimum number of points to form a cluster were set to be 50 m and 2 respectively in this study, based on recommended settings in prior research that used similar dataset [63]. The DBSCAN algorithm was applied to the studied dataset, which generated a number of geolocation clusters for each individual. Second, as these geolocation clusters included geolocation records from different visits paid by the same individual, they represented spots where the individual stopped, regardless of how long the individual stayed there, therefore, some of the geolocation clusters could be associated with occasional pauses, such as waiting at crossroads or getting caught in traffic jams might be contained [58,59]. In order to exclude those pauses and extract real

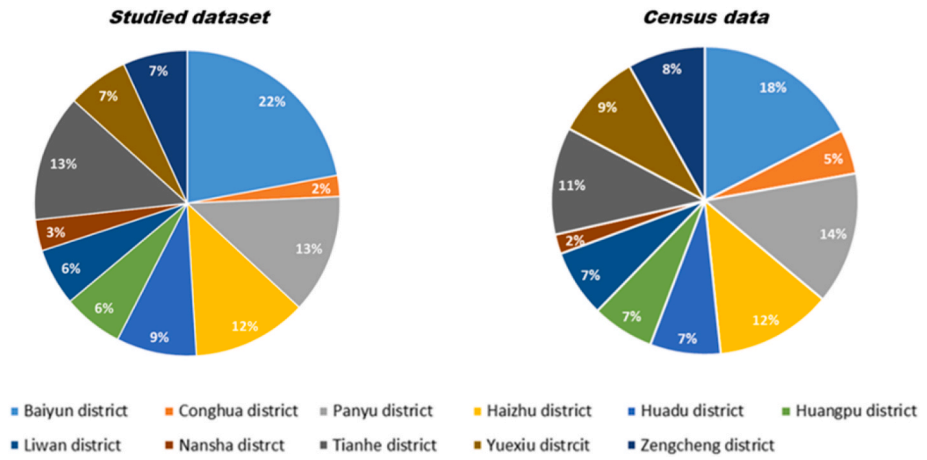

Fig. 2. Spatial distributions of the population in the studied dataset and census data.

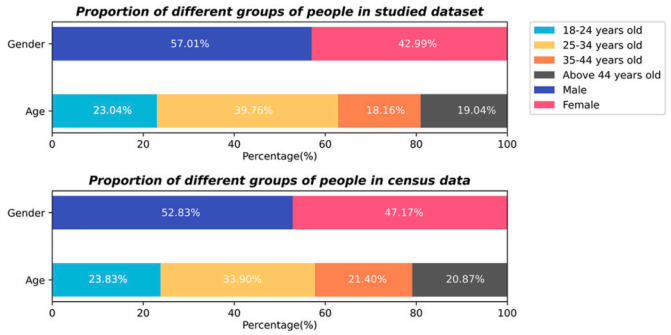

Fig. 3. Gender and age distributions of population in the studied dataset and census data.

visited locations for each individual, geolocation clusters where an individual never stayed for more than 5 min during a single visit were removed [59,64]. Finally, the each remaining geolocation cluster was considered to represent a unique visited location, whose coordinates were determined by the centroid of the corresponding geolocation cluster.

After the visited locations were extracted, the arrival time and departure time of each visitation, as well as every trip made by each individual during the study period were identified, a few samples of which are shown in Table 3. Then, the visitation frequency and waiting time of each visited location during the study period were calculated, a few samples of which are shown in Table 4.

5. Results

5.1. Individual mobility perturbation

All metrics in Table 1 were calculated for every individual in the dataset and for each week (from Wednesday to Sunday) over the study period. For each individual, the average weekly value of each metric during typhoon-free time was calculated and used to represent its normal state, while its weekly value during the typhoon events was used to represent its perturbed state. The descriptive statistics of all metrics in normal state and perturbed state are summarized in Table 5, respectively. The KS test and Wilcoxon rank-sum test results, as reported in Table 6, showed that distributions and mean values of all metrics exhibited significant changes during the typhoon week, suggesting that the typhoon events caused substantial perturbations to the mobility of the studied individuals in Guangzhou.

More specifically, for visited locations, as shown in Fig. 4a, the metrics l, f_b, f_1, f_2 and f_5 followed heavy-tail distribution in both normal state and perturbed state. However, the proportion of individuals with fewer visited locations and lower visitation frequency increased during the typhoon week, resulting in remarkable deviation in distributions of the metrics. It was also discovered that on average people tended to visit fewer places and make fewer travels due to the influence of typhoon (Fig. 4b). Fig. 4c, which shows the trajectories of a typical individual under normal conditions and during the typhoon week, illustrates how the characteristic of visited locations could be perturbed by the typhoon events.

The perturbation in movement range is illustrated in Fig. 5. It was discovered that the distribution of R_g during typhoon week shifted leftward and the number of individuals with lower R_g increased (Fig. 5a and b), which indicated that, when influenced by typhoon, individuals' movement range became relatively restricted. This phenomenon is further illustrated with the trajectories of a typical individual in Fig. 5c.

As for the perturbation in waiting time, the mean values of all related metrics, including t_t, t_h, t_1, t_2 and t_5, notably decreased (Fig. 6b), although the distributions of these metrics followed similar trend (Fig. 6a). The result suggested that people tended to spend more time staying indoors and less time travelling during the typhoon week.

According to Table 7, further analysis of the magnitude of individual mobility perturbation showed that, when influenced by Typhoons Hato and Pakhar, studied individuals in Guangzhou exhibited 7.56% decrease in the number of visited locations, 9.9% decrease in visitation frequency, 17.19% decrease in movement range and 0.57% increase in waiting time. It was also discovered that individuals' recurrent mobility, reflected by r_{f1}, r_{f2}, r_{f5}, r_{t1}, r_{t2} and r_{t5}, was affected by the typhoon events. It should be noted that the mean value of r_{ft} was larger than that of r_{f1}, r_{f2} and r_{f5}, while the mean value of r_{tt} was smaller than that of r_{t1}, r_{t2} and r_{t5}. This suggested

Table 3
Examples of trip records for ID ***f341.

Visited Location	Arrival time	Departure time	Longitude	Latitude
0	170802093354	170802113230	113.3219	23.1999
1	170802235318	170803085008	113.3009	23.2339
0	170803092624	170803204135	113.3219	23.1999
1	170803213625	170804083624	113.3009	23.2339
0	170804092133	170804130738	113.3219	23.1999
2	170804143447	170804153324	113.3217	23.1971
…	…	…	…	…

Table 4
Visitation frequency and waiting time of each location for ID ***f341.

Visited Location	Visitation Frequency	Waiting Time	Longitude	Latitude
0	28	1741891	113.3009	23.2339
1	51	1530888	113.3219	23.1999
2	3	12290	113.3217	23.1971
6	10	12125	113.3197	23.1994
26	3	10254	113.315	23.12
45	2	9632	113.3230	23.1903
…	…	…	…	…

Table 5
Descriptive statistics of metrics characterizing individual mobility pattern.

Metric	M	SD	$Q_{.25}$	$Q_{.75}$	Maximum	Minimum
Normal state						
l	8.319	7.704	3.75	10.5	169.714	1
$f_t(count)$	31.153	34.855	12.167	37.857	905.8	1
$f_1(count)$	10.954	12.464	5.25	12.25	417.2	1
$f_2(count)$	17.722	19.782	8	20.5	496.2	1
$f_5(count)$	23.603	26.013	10.333	27.857	634.4	1
$R_g(m)$	2775.551	3149.115	596.790	3849.658	35999.290	0
$t_t(s)$	360837.106	53485.055	331552.714	401034.286	432000	64563
$t_h(s)$	280869.824	91686.477	207654.8	364688.857	432000	55690.25
$t_1(s)$	280800.191	91786.392	207617.2	364688.857	432000	34790.857
$t_2(s)$	335056.154	68490.174	290966.167	389736.8	432000	47716.8
$t_5(s)$	353477.913	57340.099	319936.714	397281.0	432000	60765.4
Perturbed state						
l	7.628	8.012	3	10	178	1
$f_t(time)$	28.076	39.870	9	34	1204	1
$f_1(time)$	10.421	15.208	4	11	526	1
$f_2(time)$	16.890	23.544	6	19	694	1
$f_5(time)$	22.429	30.937	8	25	1004	1
$R_g(m)$	2651.954	4000.283	268.905	3441.415	49278.739	0
$t_t(s)$	366280.478	59991.620	335137	412649	432000	70751
$t_h(s)$	288729.499	101247.398	208080	387934	432000	54012
$t_1(s)$	288702.681	102757.405	207960	387864	432000	36123.243
$t_2(s)$	345267.196	76479.523	295234	4069235	432000	63930
$t_5(s)$	359704.665	64107.925	324093	410371	432000	69117

Note: M = mean value; SD = standard deviation; Q.25 and Q.75 represent the upper and lower quartile of the value of metrics, respectively.

Table 6
KS test and Wilcoxon rank-sum test results.

	Metric	KS test			Wilcoxon rank-sum test	
		Statistic	p-value		Statistic	p-value
Visited Location	L	0.1259	0.0	4.51e8		0.0***
	f_t	0.1527	0.0	4.86e8		0.0***
	f_1	0.1130	3.78e-299	5.03e8		0.0***
	f_2	0.1038	2.24e-252	5.03e8		0.0***
	f_5	0.1015	2.16e-241	4.85e8		0.0***
Movement Range	R_g	0.1408	0.0	4.82e8		0.0***
Waiting Time	t_t	0.1019	2.43e-243	5.23e8		0.0***
	t_h	0.0885	8.87e-184	5.56e8		0.0***
	t_1	0.0885	8.87e-184	5.55e8		0.0***
	t_2	0.0926	2.34e-201	5.29e8		0.0***
	t_5	0.1012	2.43e-243	5.21e8		0.0***

Note: $p < 0.05$ *; $p < 0.01$ **; $p < 0.001$ ***.

that, compared to individuals' overall mobility pattern, their recurrent mobility showed a weaker perturbation in visitation frequency but a greater perturbation in waiting time. In addition, the mean value of metric $Dist_{dtw}$ was 0.0607, which suggested that individual's daily movement status varied by 6.07% on average, indicating there was notable influence of typhoon events on individual's daily schedules.

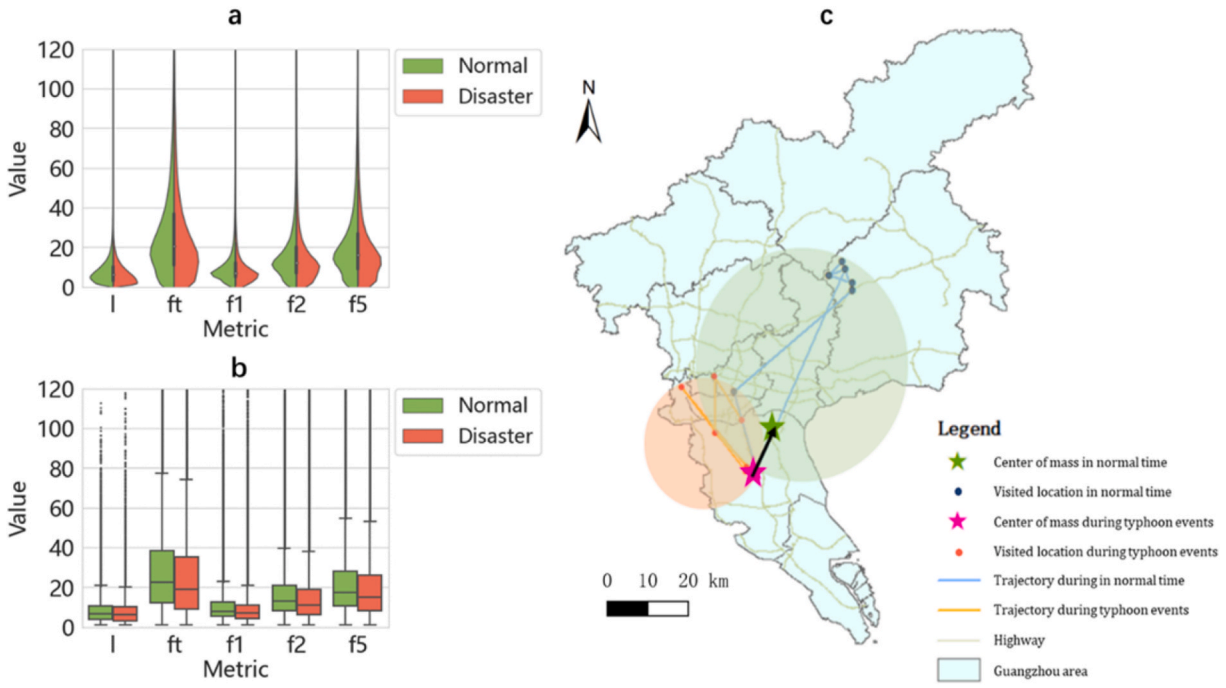

Fig. 4. The perturbation of individual mobility pattern in terms of visited locations.

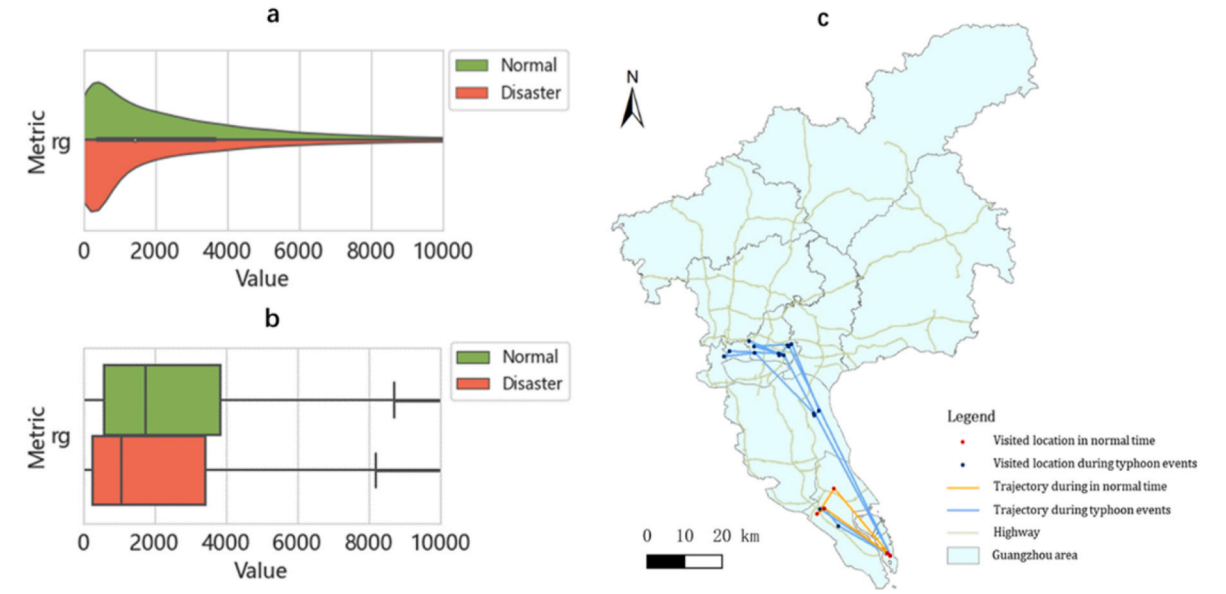

Fig. 5. The perturbation of individual mobility pattern in terms of movement range.

5.2. Individual variation of mobility perturbations

Based on the six independent variables (three categorical variables and three numerical variables) introduced in Section 3.2.1, the characteristics of all individuals in the studied dataset were computed, and the results are summarized in Tables 8 and 9. The result of Kaiser-Meyer-Olkin measure was 0.7798 (>0.7) and that of Bartlett's sphericity test was 1070250.24 ($P < 0.001$), suggesting a strong correlation between some of the dependent variables. Therefore, factor analysis was conducted to reduce the number of dependent variables.

As shown in Table 10, a total of four factors were obtained based on the factor analysis result, accounting for 88.76% of the total variance. These four factors, termed based on the perspectives from which they reflected mobility perturbations, were F1 (waiting time

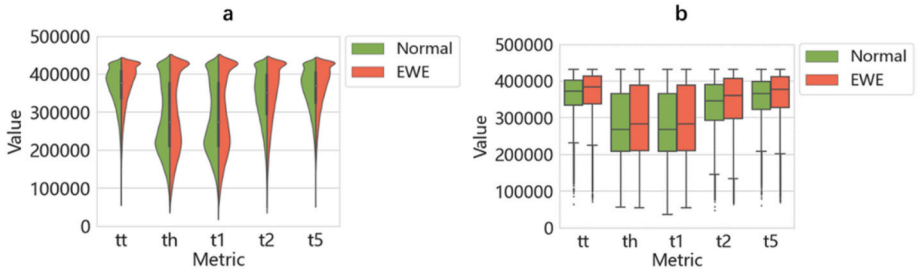

Fig. 6. The perturbation of individual mobility pattern in terms of waiting time.

Table 7
Descriptive statistics of metrics quantifying individual mobility perturbation.

Metric	M	SD	$Q_{.25}$	$Q_{.75}$
r_l	−7.56%	0.224	−21.31%	6.62%
r_{ft}	−9.90%	0.273	−23.44%	6.51%
r_{f1}	−7.41%	0.253	−20.75%	6.93%
r_{f2}	−7.53%	0.258	−20.59%	6.90%
r_{f3}	−8.25%	0.267	−21.95%	6.93%
r_{Rg}	−17.19%	0.436	−44.69%	5.91%
r_{tt}	0.57%	0.057	−1.17%	3.17%
r_{th}	0.69%	0.108	−3.32%	6.11%
r_{t1}	0.72%	0.108	−3.30%	6.13%
r_{t2}	0.78%	0.078	−1.90%	4.62%
r_{t5}	0.67%	0.062	−1.37%	3.62%
$Dist_{dtw}$	0.0607	0.039	0.0339	0.0818

Note: M = mean value; SD = standard deviation; Q.25 and Q.75 represent the upper and lower quartile of the value of metrics, respectively.

Table 8
Characteristics of individuals in the studied dataset.

Characteristic	Group	Frequency	Percentage
Gender	Male	30656	57.01%
	Female	23113	42.99%
Age	18–24	12387	23.04%
	25–34	21380	39.76%
	35–44	9762	18.16%
	45+	10240	19.04%
Travel preference	Explorer	30656	57.01%
	Returner	23113	42.99%

Table 9
Descriptive statistics for three numerical variables.

	M	SD	$Q_{.25}$	$Q_{.75}$	Maximum	Minimum
Rg (m)	2775.551	3149.115	596.790	3849.658	35999.290	0
home_to_cbd (m)	18188.639	14872.427	6798.914	26273.046	108813.052	58.617
home_to_typhoon (m)	88090.460	11831.805	80716.698	93791.090	163198.381	57650.566

Note: (1) M = mean value; SD = standard deviation; Q.25 and Q.75 represent the upper and lower quartile of the value of metrics, respectively. (2) The tracks of typhoons can be found in China Meteorological Administration's database [54].

perturbation), F2 (visitation frequency perturbation), F3 (visited location and movement range perturbation), and F4 (movement status perturbation). The descriptive statistics of these four factors are summarized in Table 11. It should be noted that a negative value of F1 represented an increase in waiting time, a negative value of F2 and F3 represented a decrease in visitation frequency, number of visited locations or movement range, and a larger value of F4 represented a greater perturbation in movement status pattern. These fours factors were used as final dependent variables in the following linear regression analysis.

The results of the multiple linear regression analysis are summarized in Tables 12–15. These results have led to several findings. First of all, mobility perturbation of females during disasters was generally greater than that of males. It could also be found that individuals aged above 45 years old had a larger mobility perturbation during the typhoon week. Second, under the influence of typhoon events, individuals' home location showed a notable impact on their waiting time perturbation and movement status perturbation (Tables 12 and 15), while showing no obvious effect on their visited location or movement range perturbations (Tables 13

Table 10
Factor analysis results.

Factor	Metrics contained in factor	Rotated component	Eigenvalue	Proportion	Cumulative
F1	r_{t_t}	−0.8908	5.7877	48.23%	48.23%
Waiting Time	r_{t_h}	−0.9001			
Perturbation	r_{t_1}	−0.9439			
	r_{t_2}	−0.9187			
	r_{t_5}	−0.8986			
F2	r_{f_t}	0.9337	2.7716	23.10%	71.33%
Visitation Frequency	r_{f_1}	0.9590			
Perturbation	r_{f_2}	0.9295			
	r_{f_5}	0.8897			
F3	r_l	0.7606	1.1567	9.64%	80.97%
Visited Location and Movement Range Perturbation	r_{R_g}	0.8885			
F4	$dist_{DTW}$	0.9724	0.0935	7.79%	88.76%
Movement Status Perturbation					

Note: Rotated component is a key output of factor analysis, which reflects estimates of the correlation between each of the metrics and the four factors.

Table 11
Descriptive statistics of four factors.

Metric	M	SD	$Q_{.25}$	$Q_{.75}$	Maximum	Minimum
F1	−0.0313	0.3515	−0.2074	0.0992	2.7784	−2.1227
F2	−0.3012	0.9325	−0.7646	0.2187	3.5583	−3.6670
F3	−0.2103	0.5007	−0.5053	0.0763	1.5223	−1.6033
F4	0.0591	0.0382	0.0330	0.0795	0.4803	0.0000

Note: M = mean value; SD = standard deviation; Q.25 and Q.75 represent the upper and lower quartile of the value of metrics, respectively.

Table 12
Multiple linear regression analysis result for F1 (waiting time perturbation).

Variable	Coefficient	Standard error	t	p-value	95% CI
gender[*male*]	0.0089	0.003	2.868	0.004**	(0.003, 0.015)
age[25 − 34]	−0.0066	0.004	−1.657	0.098	(-0.014, 0.001)
age[35 − 44]	−0.0118	0.005	−2.473	0.013*	(-0.021, −0.002)
age[45 +]	−0.0142	0.005	−2.994	0.003**	(-0.024, −0.005)
type[*returner*]	0.0106	0.003	3.481	0.001**	(0.005, 0.017)
rg	−5.62e-6	4.88e-7	−11.506	0.000***	(-6.57e-6, -4.66e-6)
*home*_to_cbd	−1.35e-7	1.28e-7	−1.054	0.292	(-3.85e-7, 1.16e-7)
home_to_typhoon	8.88e-7	1.59e-7	5.571	0.000***	(5.76e-7, 1.20e-6)

Note: Number of observations = 53769; Adjusted R-squared = 0.003.
$p < 0.05$ *; $p < 0.01$ **; $p < 0.001$ ***.

Table 13
The results of multiple linear regression for F2 (visitation frequency perturbation).

Variable	Coefficient	Standard error	t	p-value	95% CI
gender[*male*]	0.0332	0.008	4.014	0.000**	(0.017, 0.049)
age[25 − 34]	0.0249	0.011	2.357	0.018*	(0.004, 0.046)
age[35 − 44]	0.0059	0.013	0.466	0.641	(-0.019, 0.031)
age[45 +]	−0.0133	0.013	−1.057	0.291	(-0.038, 0.011)
type[*returner*]	0.0142	0.008	1.753	0.080	(-0.002, 0.030)
rg	−5.88e-6	1.30e-6	4.531	0.000***	(3.33e-6, 8.42e-6)
*home*_to_cbd	−1.20e-7	3.39e-7	−0.353	0.724	(-7.84e-7, 5.45e-7)
home_to_typhoon	7.62e-7	4.24e-7	1.798	0.072	(-6.84e-8, 1.59e-6)

Note: Number of observations = 53769; Adjusted R-squared = 0.001.
$p < 0.05$ *; $p < 0.01$ **; $p < 0.001$ ***.

Table 14
The results of multiple linear regression for F3 (visited location and movement range perturbation).

Variable	Coefficient	Standard error	t	p-value	95% CI
gender[*male*]	0.0224	0.004	5.074	0.000***	(0.014, 0.031)
age[25 − 34]	0.0380	0.006	6.729	0.000***	(0.027, 0.049)
age[35 − 44]	0.0414	0.007	6.106	0.000***	0.028, 0.055)
age[45 +]	0.0066	0.007	0.981	0.327	(-0.007, 0.020)
type[*returner*]	0.0934	0.004	21.513	0.000***	(0.085, 0.102)
rg	−3.5e-6	6.93e-7	−5.050	0.000***	(-4.86e-6, -2.14e-6)
home_to_cbd	−1.13e-9	1.81e-7	−0.006	0.995	(-3.56e-7, 3.54e-7)
home_to_typhoon	2.73e-7	2.26e-7	1.207	0.228	(-1.71e-7, 7.17e-7)

Note: Number of observations = 53769; Adjusted R-squared = 0.010.
$p < 0.05$ *; $p < 0.01$ **; $p < 0.001$ ***.

Table 15
The results of multiple linear regression for F4 (movement status perturbation).

Variable	Coefficient	Standard error	t	p-value	95% CI
gender[*male*]	0.0073	0.000	22.973	0.000***	(0.007, 0.008)
age[25 − 34]	−0.0040	0.000	−9.747	0.000***	(-0.005, −0.003)
age[35 − 44]	−0.0062	0.000	−12.709	0.000***	(-0.007, −0.005)
age[45 +]	−0.0119	0.000	−24.499	0.000***	(-0.013, −0.011)
type[*returner*]	−0.0097	0.000	−30.890	0.000***	(-0.010, −0.009)
rg	2.89e-6	5.01e-8	57.652	0.000***	(2.79e-6, 2.99e-6)
home_to_cbd	2.86e-7	1.31e-8	21.825	0.000***	(2.60e-7, 3.12e-7)
home_to_typhoon	−3.72e-8	1.64e-8	−2.275	0.023*	(-6.93e-8, -5.16e-9)

Note: Number of observations = 53769; Adjusted R-squared = 0.109.
$p < 0.05$ *; $p < 0.01$ **; $p < 0.001$ ***.

and 14). It was found that the further an individual lived away from the CBD, the more significantly his/her movement status was influenced by the typhoon events (Table 15); the closer the individual lived to the center of typhoon tracks, the more significantly his/her waiting time increased (Table 12). Third, individuals' *Rg* in normal time had a significant impact on all dependent variables (all $p < 0.001$ in Tables 12–15), which suggested that individuals who preferred distant movements experienced a more intense mobility perturbation during the typhoon week. In addition, the mobility perturbation of explorers was greater than that of returners, especially in terms of the movement range and number of visited locations (Table 14).

Besides analyzing the relationship between individual's characteristics and individual mobility perturbation, this study also revealed the individual variation of mobility perturbation by clustering individuals into several groups. K-means clustering algorithm was adopted in this study. Individuals' mobility perturbations were characterized by a four-dimensional variable composed of four factors introduced above, namely vector *(F1, F2, F3, F4)*, based on which the k-means clustering algorithm was computed. To determine the number of clusters *k*, this study adopted the Elbow method explained in Section 3.3.3. As shown in Fig. 7, the part of the line graph where $k < 4$ was steeply declining, while the part where $k < 4$ was much smoother. Therefore, in this study, k-means

Fig. 7. The relationship between the number of clusters (k) and distortion.

Table 16
The results of k-means clustering.

Cluster	Proportion of the population	Characteristics of individuals' mobility perturbation			
		F1 (M)	F2 (M)	F3 (M)	F4 (M)
1	13.77%	0.2167	1.0885	0.0400	0.0733
2	29.51%	−0.1287	−0.8187	−0.3442	0.0540
3	9.98%	−0.2481	−2.1568	−0.8231	0.0427
4	46.74%	0.0033	0.0123	−0.0686	0.0615

Note: M means mean value.

clustering algorithm was performed with k = 4. The results are shown in Table 16.

Four clusters were extracted, which contained 29.74%, 14.03%, 10.00% and 46.24% of the studied individuals respectively. As shown in Table 16, the mean values of F1, F2, F3 and F4 for individuals belonging to *Cluster 4* were close to zero, indicating a slight perturbation of individual mobility pattern during EWEs. Individuals who belonged to *Cluster 2* and *Cluster 3* all possessed negative values of F1, F2 and F3, but the mobility perturbation of individuals in Cluster 3 was much greater than that of individuals in Cluster 2. As for individuals in *Cluster 1*, their mobility perturbations showed a different pattern. They possessed positive values of F1, F2 and F3, reflecting an increase in visitation frequency and number of locations, but a decrease in waiting time during EWEs.

The above results showed strong variations in individuals' mobility perturbation, indicating that there existed different patterns of responses to EWE-induced impacts among the population. Specifically, a large proportion of individuals belonged to *Cluster 4* whose mobility was only slightly influenced by EWEs. Around 10% of individuals belong to *Cluster 3* and were vulnerable to the impact of EWEs. They tended to visit few places, make fewer travels and spend more time staying indoors during EWEs and their movement ranges were also largely restricted, just as what was observed in Section 5.1 and Table 11. Comparatively, individuals belonging to *Cluster 2* who accounted for 29.51% of the total population also showed similar patterns of perturbations in their mobility. However, the magnitude of their mobility perturbation was much smaller than that of individuals in *Cluster 3*. Meanwhile, individuals in Cluster 1 showed different characteristics in their mobility perturbations. They tended to visit more places and make more travels, and they had shorter waiting time during EWEs.

6. Discussions

This study proposed a three-module analytical framework for characterizing individual mobility perturbations during EWEs, and demonstrated its efficacy by applying it to investigate the impact of Typhoons Hato and Pakhar on the mobility of citizens in the city of Guangzhou. Based on the results of the case study, the following three findings could be drawn. First, while prior studies have reported that people's travel length and radius of gyration would be significantly perturbed under EWEs [17,65], this study found that EWEs could also cause notable perturbations in individuals' visited locations and waiting time. Specifically, the case study results suggest that individuals' number of visited locations and visitation frequency tend to decrease while their waiting time tend to increase during EWEs. This reflects an overall reduction in traffic demand and people's travel intention during EWEs, and corroborates with prior studies that reported similar phenomenon. For instance, prior studies have observed the reduction of traffic volumes and the change on traffic demand due to extreme weathers such as cold and snow [66,67]. Second, the results showed that individuals' movement status also changed during the EWEs. The perturbation of movement status reflects the influence of EWEs on individuals' daily life. During EWEs, they may have to adjust their schedules and minimize travels, due to e.g. the collapse of transportation systems, closure of schools and offices, or concerns over personal safety [67,68]. Third, by comparing different aspects of the assessed individual mobility perturbation, it was found that individuals' recurrent mobility showed a weaker perturbation in visitation frequency but a greater perturbation in waiting time. It indicates that people are more likely to visit and stay in their familiar places, namely places they frequently visited in normal conditions, when under the influence of EWEs. More importantly, this finding also suggests that frequently visited locations not only characterize people's mobility pattern in steady states [24,31,69], but also play an important role in shaping people's perturbed mobility patterns.

The investigation of the correlation between individuals' characteristics and their mobility perturbation also leads to new insights about individual mobility perturbations. For example, as aforementioned, the results showed that the further one lived to the CBD, the more significantly his/her movement status was influenced by the typhoon events. This finding suggests that there is remarkable variation in mobility perturbations experienced by people living in different regions in a city, which highlights the significance of spatial heterogeneity of EWE-induced impact [39] and human mobility resilience [70]. A possible explanation of such spatial heterogeneity could be that people who live further from the CBD usually have long-distance commutes every day, and their routine travels are more easily affected by EWEs. In addition, the spatial heterogeneity of EWE-induced individual mobility perturbation may also be attributed to the imbalanced accessibility to infrastructure and various essential services in cities [38]. For instance, prior research has found that recreational and commercial trips tend to be more severely influenced than commuting trips [71]. Therefore, people living in suburban areas, who are more likely to have less accessibility to recreational and commercial facilities than those living in the downtown areas and hence have to travel longer to access these services, become more vulnerable to EWE-induced impacts. Another important finding of this study is that, the perturbed individual mobility pattern during EWEs possesses a certain degree of predictability. It was found in this study that *Rg* in normal time had a significant impact on individual mobility perturbation, which is aligned with similar findings reported by prior research [20]. This study also revealed for the first time in the literature that the mobility perturbation of individuals who were categorized as explorers based on their regular mobility patterns was greater than

the mobility perturbation of returners, especially in terms of movement range and number of visited locations. The above correlations between individuals' mobility perturbations and their mobility pattern in normal time indicate the possibility of predicting human mobility during EWEs based on human mobility data collected in normal time.

The findings of this study also bear a few important implications for urban planning and crisis management. First, as prior research has pointed out, knowledge about human mobility perturbation can be used to inform the estimation of EWE impacts [72]. Specifically, the proposed analytical framework could facilitate policy maker with assessing the magnitudes of EWE impacts, determining the spatial distribution of the impacts within city boundaries, and evaluating the effectiveness of particular risk reduction policies, which could promote the optimal allocation of emergency response resources and urban mobility planning in the aftermath of EWEs. Also, by linking individual mobility perturbations to important public entities, city managers could foresee whether critical public services could be assured during EWEs and take proper emergency response measures accordingly. Third, in line with prior research that found individual characteristics to be associated with people's reaction to extreme events [40,70,73], this study reveals that mobility perturbation varies among individuals with different characteristics and clusters individuals into several groups with different responses to EWEs. As such, the proposed analytical framework provides policy makers with a possible tool to predict people's mobility perturbation based on their demographic attributes, home location and travel preference, and hence identify those who are vulnerable to EWE-induced impacts. These people could therefore be prioritized in risk mitigation measures. Lastly, this study also highlights the spatial heterogeneity of EWE-induced impact that is partially attributed to people's imbalanced accessibility to infrastructure and various essential services in different regions of the city. This not only informs policy makers of the potential existence of social inequity in terms of the resilience to EWE impacts, which should be considered in EWE impact mitigation strategies, but also suggests that these strategies need to be incorporated in the long-term urban planning practices. For example, this study reveals that individuals living in suburban exhibit greater mobility perturbation, due the long-distance commutes and the lack of recreational and commercial facilities in their neighborhood. This calls for providing more transportation infrastructure and services to improve accessibility in suburban areas and balancing jobs-housing relationship and housing supply between suburbs and city centers to reduce city-wide commuting distance [13]. Meanwhile, the results also suggest that a polycentric urban structure is more resilient than a monocentric one [74]. Above all, urban planners and policy makers could incorporate the knowledge of EWE-induced mobility perturbation into the urban development scheme and risk reduction strategies to enhance urban resilience.

7. Conclusions

EWEs are significant threats to urban regions. Urban human mobility, as a fundamental component of the urban system, is sensitive to such impact and shows perturbation in its spatial-temporal characteristics under the influence of EWEs. This study proposed an analytical framework for characterizing individual mobility perturbation under EWEs. The proposed framework is composed of three modules that are designed to capture individual mobility patterns, assess individual mobility perturbations, and examine the correlations between individuals' characteristics and their mobility perturbations. The findings of this study demonstrated that: (1) individual mobility pattern exhibited significant changes under the influence of EWEs. To be more specific, individuals would experience decreases in the number of visited locations, visitation frequency and movement range, increases in waiting time, and changes in movement status pattern; (2) individuals' recurrent mobility, compared with their overall mobility pattern, showed weaker perturbation in visitation frequency but greater perturbation in waiting time during EWEs; and (3) individuals' mobility perturbation closely correlated with their characteristics including demographic attributes, home location and travel preference.

The contributions of this study are multifold. First, it expands the connotation of individual mobility perturbation by integrating a wide range of spatial-temporal characteristics and provides a manifold understanding of individual mobility perturbation and the affected city functioning under the influence of EWEs. Meanwhile, this study also contributes to assessing individual mobility perturbation. The methods proposed in the analytical framework could be used to compare EWE impact between different regions or extreme events, the results of which could inform urban crisis management and resilience enhancement. Moreover, this study reveals possible influencing factors of individual mobility perturbation, which offers possible explanations of why people's mobility patterns would be perturbed during EWEs and why the perturbations may vary among individuals. Also, by clustering individuals into several groups according to their mobility perturbation, this study demonstrates the existence of different patterns of responses to EWE-induced impact among individuals. The above advancement of knowledge on human mobility lays solid foundation for future research to further look into the modeling and prediction of EWE-perturbed urban human mobility. Practically, the knowledge of individual mobility pattern under the impact of EWEs could enable policy makers to identify vulnerable individuals and prioritize their protection, predict urban mobility during EWEs, select effective emergency response measures, and implement resilience oriented urban planning, which are all important issues for improved safety of cities and their residents during EWEs.

This study bears three limitations that are noteworthy. First, due to the constrain of regulations, individuals under 18 years old were not included in the analysis. However, as a potentially vulnerable group, their mobility perturbation should be analyzed by future studies if possible. Second, the adjusted R-square was relatively small in the regression analysis results, which indicated that using the independent variables in the regression model alone could not fully interpret or accurately predict the individual mobility perturbation. To develop an accurate prediction model of the individual mobility perturbation, future studies could adopt more variables to

describe individual characteristics when granular data are made available. For example, when characterizing demographic attributes, in addition to gender and age, other key factors such as class, occupation and economic situation could also be investigated. Third, this study mainly focused on the relationship between individual's characteristics and mobility perturbation, but how one's characteristics influence his or her mobility perturbation still requires further exploration. Future efforts could be made to study the underlying influence mechanisms of these factors on individual mobility perturbation, which could lead to deeper understanding of and better ways to model and predict individuals' behaviors under the influence of the EWEs.

To sum up, by investigating EWE-induced individual mobility perturbation in cities, this study provides a new perspective to understand the multifaceted influences of EWEs in urban regions, including the failure of urban infrastructure system, the anomaly of socio-economic activities and people's perturbed behavioral patterns. The findings in this study could potentially provide guidance for urban planning and crisis management. Firstly, a quantitative measurement of individual mobility perturbation is proposed in this study, providing foundation for EWE-induced impacts estimation and risk reduction policy evaluation, which could improve emergency response and urban mobility planning in cities. Moreover, by looking into the individual variation of mobility perturbation, the analytical framework proposed in this study could help policy makers to identify the most vulnerable groups under the impacts of EWEs and offers an example that the knowledge about individual mobility perturbation could ultimately advance urban resilience.

Declaration of competing interest

The authors declare that they have no known competing financial interests or personal relationships that could have appeared to influence the work reported in this paper.

Acknowledgments

This material is based upon work supported by the National Natural Science Foundation of China (NSFC) under Grant No. 71974105. The authors are grateful for the support of the NSFC. Any opinions, findings, conclusions or recommendations expressed in the paper are those of the authors and do not necessarily reflect the views of the funding agency.

References

[1] A.H. Sobel, M.K. Tippett, Extreme Events: Trends and Risk Assessment Methodologies, Resilience, Elsevier Inc., 2018, pp. 3–12, https://doi.org/10.1016/b978-0-12-811891-7.00001-3.
[2] P. Stott, How climate change affects extreme weather events, Science 352 (2016) 1517–1518, https://doi.org/10.1126/science.aaf7271.
[3] S. Mahmood, A. ul H. Khan, S. Ullah, Assessment of 2010 flash flood causes and associated damages in Dir Valley, Khyber Pakhtunkhwa Pakistan, Int. J. Disaster Risk Reduc. 16 (2016) 215–223, https://doi.org/10.1016/j.ijdrr.2016.02.009.
[4] L. Bakkensen, E. Franco, G.M. Garfin, Z. Adeel, A. María, R.A. Mcpherson, M. Karla, M. Blanche, H. Saffari, X. Wen, Developing a comprehensive methodology for evaluating economic impacts of floods in Canada, Mexico and the United States, Int. J. Disaster Risk Reduc. 50 (2020), https://doi.org/10.1016/j.ijdrr.2020.101861.
[5] J. Moreno, D. Shaw, Community resilience to power outages after disaster: a case study of the 2010 Chile earthquake and tsunami, Int. J. Disaster Risk Reduc. 34 (2019) 448–458, https://doi.org/10.1016/j.ijdrr.2018.12.016.
[6] Y. Finzi, N. Ganz, Y. Limon, S. Langer, The next big earthquake may inflict a multi-hazard crisis – insights from COVID-19, extreme weather and resilience in peripheral cities of Israel, Int. J. Disaster Risk Reduc. 61 (2021) 102365, https://doi.org/10.1016/j.ijdrr.2021.102365.
[7] T.-Y. Ling, Y.-C. Chiang, Strengthening the resilience of urban retailers towards flood risks - a case study in the riverbank region of Kaohsiung City, Int. J. Disaster Risk Reduc. 27 (2018) 541–555, https://doi.org/10.1016/j.ijdrr.2017.11.020.
[8] O.B. Jensen, Staging Mobilities, Routledge, 2013.
[9] C. Kang, X. Ma, D. Tong, Y. Liu, Intra-urban human mobility patterns: an urban morphology perspective, Phys. A Stat. Mech. Its Appl. 391 (2012) 1702–1717, https://doi.org/10.1016/j.physa.2011.11.005.
[10] A. Rahimi-Golkhandan, M.J. Garvin, Q. Wang, Assessing the impact of transportation diversity on postdisaster intraurban mobility, J. Manag. Eng. 37 (2021), 04020106, https://doi.org/10.1061/(ASCE)ME.1943-5479.0000872.
[11] X. Li, G. Pan, Z. Wu, G. Qi, S. Li, D. Zhang, W. Zhang, Z. Wang, Prediction of urban human mobility using large-scale taxi traces and its applications, Front. Comput. Sci. China 6 (2012) 111–121, https://doi.org/10.1007/s11704-011-1192-6.
[12] P. Pucci, Mobility practices as a knowledge and design tool for urban policy, in: P. Pucci, M. Colleoni (Eds.), Underst. Mobilities Des. Contemp. Cities, Springer International Publishing, Cham, 2016, pp. 3–21, https://doi.org/10.1007/978-3-319-22578-4_1.
[13] T. Yang, Understanding commuting patterns and changes: counterfactual analysis in a planning support framework, Environ. Plan. B Urban Anal. City Sci. 47 (2020) 1440–1455, https://doi.org/10.1177/2399808320924433.
[14] Q. Huang, D.W.S. Wong, Activity patterns, socioeconomic status and urban spatial structure: what can social media data tell us? Int. J. Geogr. Inf. Sci. 30 (2016) 1873–1898, https://doi.org/10.1080/13658816.2016.1145225.
[15] Q. Wang, J.E. Taylor, Quantifying human mobility perturbation and resilience in hurricane Sandy, PLoS One 9 (2014), e112608, https://doi.org/10.1371/journal.pone.0112608.
[16] F. Zhang, Z. Li, N. Li, D. Fang, Assessment of urban human mobility perturbation under extreme weather events: a case study in Nanjing, China, Sustain. Cities Soc. 50 (2019) 101671, https://doi.org/10.1016/j.scs.2019.101671.
[17] W. Qi, T. John E, Quantifying, comparing human mobility perturbation during hurricane Sandy, typhoon wipha, typhoon haiyan, procedia econ, Financ. Times 18 (2014) 33–38, https://doi.org/10.1016/s2212-5671(14)00910-1.
[18] T. Yabe, K. Tsubouchi, A. Sudo, Y. Sekimoto, A framework for evacuation hotspot detection after large scale disasters using location data from smartphones: case study of Kumamoto Earthquake, GIS Proc. ACM Int. Symp. Adv. Geogr. Inf. Syst. (2016), https://doi.org/10.1145/2996913.2997014.
[19] Y. Wang, Q. Wang, J.E. Taylor, Aggregated responses of human mobility to severe winter storms: an empirical study, PLoS One 12 (2017) 1–15, https://doi.org/10.1371/journal.pone.0188734.
[20] Q. Wang, J.E. Taylor, Patterns and limitations of urban human mobility resilience under the influence of multiple types of natural disaster, PLoS One 11 (2016), e0147299, https://doi.org/10.1371/journal.pone.0147299.
[21] T. Horanont, S. Phithakkitnukoon, T.W. Leong, Y. Sekimoto, R. Shibasaki, Weather effects on the patterns of people's everyday activities: a study using GPS traces of mobile phone users, PLoS One 8 (2013) 1–14, https://doi.org/10.1371/journal.pone.0081153.
[22] C.L. Gray, V. Mueller, Natural disasters and population mobility in Bangladesh, Proc. Natl. Acad. Sci. U.S.A. 109 (2012) 6000–6005, https://doi.org/10.1073/pnas.1115944109.
[23] T. Bhattacharya, L. Kulik, J. Bailey, Extracting significant places from mobile user GPS trajectories: a bearing change based approach, GIS Proc. ACM Int. Symp. Adv. Geogr. Inf. Syst. (2012) 398–401, https://doi.org/10.1145/2424321.2424374.

[24] M.C. González, C.A. Hidalgo, A.L. Barabási, Understanding individual human mobility patterns, Nature 453 (2008) 779–782, https://doi.org/10.1038/nature06958.
[25] A. Schafer, Regularities in travel demand: an international perspective, J. Transport. Stat. 3 (2000), https://doi.org/10.21949/1501657.
[26] D. Brockmann, L. Hufnagel, T. Geisel, The scaling laws of human travel, Nature 439 (2006) 1–9.
[27] E.W. Montroll, G.H. Weiss, Random walks on lattices. II, J. Math. Phys. 6 (1965) 167–181, https://doi.org/10.1063/1.1704269.
[28] C. Song, T. Koren, P. Wang, A.-L. Barabási, Modelling the scaling properties of human mobility, Nat. Phys. 6 (2010) 818–823, https://doi.org/10.1038/nphys1760.
[29] L. Pappalardo, F. Simini, S. Rinzivillo, D. Pedreschi, F. Giannotti, A.L. Barabási, Returners and explorers dichotomy in human mobility, Nat. Commun. 6 (2015) 1–8, https://doi.org/10.1038/ncomms9166.
[30] H. Barbosa, F.B. de Lima-Neto, A. Evsukoff, R. Menezes, The effect of recency to human mobility, EPJ Data Sci 4 (2015) 1–14, https://doi.org/10.1140/epjds/s13688-015-0059-8.
[31] C. Song, Z. Qu, N. Blumm, A.L. Barabási, Limits of predictability in human mobility, Science 327 (2010) 1018–1021, https://doi.org/10.1126/science.1177170.
[32] C.M. Schneider, V. Belik, T. Couronné, Z. Smoreda, M.C. González, Unravelling daily human mobility motifs, J. R. Soc. Interface 10 (2013) 20130246, https://doi.org/10.1098/rsif.2013.0246.
[33] Y. Wang, J.E. Taylor, Tracking urban resilience to disasters: a mobility network-based approach, Proc. Int. ISCRAM Conf. (2017) 97–109.
[34] Q. Wang, J.E. Taylor, Data-driven simulation of urban human mobility constrained by natural disasters, Proc. - Winter Simul. Conf. (2016) 3357–3364, https://doi.org/10.1109/WSC.2016.7822366, 0.
[35] C. Kang, S. Gao, X. Lin, Y. Xiao, Y. Yuan, Y. Liu, X. Ma, Analyzing and geo-visualizing individual human mobility patterns using mobile call records, in: 2010 18th Int. Conf. Geoinformatics, Geoinformatics, vol. 2010, 2010, https://doi.org/10.1109/GEOINFORMATICS.2010.5567857.
[36] Q. Wang, N.E. Phillips, M.L. Small, R.J. Sampson, Urban mobility and neighborhood isolation in America's 50 largest cities, Proc. Natl. Acad. Sci. U.S.A. 115 (2018) 7735–7740, https://doi.org/10.1073/pnas.1802537115.
[37] J.P. Bagrow, Y.R. Lin, Mesoscopic structure and social aspects of human mobility, PLoS One 7 (2012), https://doi.org/10.1371/journal.pone.0037676.
[38] Y. Xu, S.-L. Shaw, Z. Zhao, L. Yin, Z. Fang, Q. Li, Understanding aggregate human mobility patterns using passive mobile phone location data: a home-based approach, Transportation 42 (2015) 625–646, https://doi.org/10.1007/s11116-015-9597-y.
[39] K. Huang, Mapping the hazard: visual analysis of flood impact on urban mobility, IEEE Comput. Graph. Appl. 41 (2021) 26–34, https://doi.org/10.1109/MCG.2020.3041371.
[40] E.J. Baker, Household preparedness for the aftermath of hurricanes in Florida, Appl. Geogr. 31 (2011) 46–52, https://doi.org/10.1016/j.apgeog.2010.05.002.
[41] E.E. Koks, B. Jongman, T.G. Husby, W.J.W. Botzen, Combining hazard, exposure and social vulnerability to provide lessons for flood risk management, Environ. Sci. Pol. 47 (2015) 42–52, https://doi.org/10.1016/j.envsci.2014.10.013.
[42] S. Hasan, C.M. Schneider, S.V. Ukkusuri, M.C. González, Spatiotemporal patterns of urban human mobility, J. Stat. Phys. 151 (2013) 304–318, https://doi.org/10.1007/s10955-012-0645-0.
[43] I.T. Young, Proof without prejudice: use of the Kolmogorov Smirnov test for the analysis of histograms from flow systems and other sources, J. Histochem. Cytochem. 25 (1977) 935–941, https://doi.org/10.1177/25.7.894009.
[44] F. Wilcoxon, Individual comparisons by ranking methods, Biometrics Bull. 1 (1945) 80–83, https://doi.org/10.2307/3001968.
[45] A.C.B. Da Costa Filho, J.P. De Brito Filho, R.E. De Araujo, C.A. Benevides, Infrared-based system for vehicle classification, SBMO/IEEE MTT-S Int. Microw. Optoelectron. Conf. Proc. (2009) 537–540, https://doi.org/10.1109/IMOC.2009.5427528.
[46] J.C. Brown, A. Hodgins-Davis, P.J.O. Miller, Classification of vocalizations of killer whales using dynamic time warping, J. Acoust. Soc. Am. 119 (2006), https://doi.org/10.1121/1.2166949. EL34–EL40.
[47] R. Wang, N. Li, Y. Wang, Does the returners and explorers dichotomy in urban human mobility depend on the observation duration? An empirical study in Guangzhou, China, Sustain. Cities Soc. 69 (2021), 102862, https://doi.org/10.1016/j.scs.2021.102862.
[48] A.I. Khuri, in: fifth ed., in: C. Douglas, Elizabeth A. Montgomery, G. Peck, Geoffrey Vining (Eds.), Introduction to Linear Regression Analysis, vol. 81, 2013, pp. 318–319, https://doi.org/10.1111/insr.12020_10.
[49] D. Knoke, Structural equation models, in: Encycl. Soc. Meas., Elsevier, 2005, pp. 689–695, https://doi.org/10.1016/B0-12-369398-5/00392-3.
[50] H.F. Kaiser, A second generation little jiffy, Psychometrika 35 (1970) 401–415, https://doi.org/10.1007/BF02291817.
[51] M.S. Bartlett, The effect of standardization on a Chi-square approximation in factor analysis, Biometrika 38 (1951) 337–344, https://doi.org/10.1093/biomet/38.3-4.337.
[52] J.A. Hartigan, M.A. Wong, A K-means clustering algorithm, J. R. Stat. Soc. Ser. C (Applied Stat. 28 (1979) 100–108, https://doi.org/10.2307/2346830.
[53] R.L. Thorndike, Who belongs in the family? Psychometrika 18 (1953) 267–276, https://doi.org/10.1007/BF02289263.
[54] M. Ying, W. Zhang, H. Yu, X. Lu, J. Feng, Y. Fan, Y. Zhu, D. Chen, An overview of the China meteorological administration tropical cyclone database, J. Atmos. Ocean. Technol. 31 (2014) 287–301, https://doi.org/10.1175/JTECH-D-12-00119.1.
[55] Typhoon Pakhar Retraces Hato's Path of Destruction, China Dly, 2017. http://www.china.org.cn/china/2017-08/28/content_41485729.htm.
[56] SE China bracing for Typhoon Hato, China Dly, 2017. http://www.chinadaily.com.cn/china/2017-08/23/content_30991217.htm.
[57] Statistics Bureau of Guangzhou Municipality, The Report of the Seventh National Census of Guangzhou, 2021. http://www.gz.gov.cn/zwgk/sjfb/tjgb/.
[58] M. Zignani, S. Gaito, G. Rossi, Extracting human mobility and social behavior from location-aware traces, Wireless Commun. Mobile Comput. 13 (2013) 313–327, https://doi.org/10.1002/wcm.2209.
[59] M. Papandrea, K. Keramat, M. Zignani, S. Gaito, S. Giordano, G. Paolo, On the properties of human mobility, Computer Communications 87 (2016) 19–36, https://doi.org/10.1016/j.comcom.2016.03.022.
[60] M. Ester, H.-P. Kriegel, J. Sander, X. Xu, A density-based algorithm for discovering clusters in large spatial databases with noise, in: Proc. 2nd Int. Conf. Knowl. Discov, . Data Min., Portland, OR, USA, 1996, pp. 226–231. https://dl.acm.org/doi/10.5555/3001460.3001507.
[61] Y. Hu, S. Gao, K. Janowicz, B. Yu, W. Li, S. Prasad, Extracting and understanding urban areas of interest using geotagged photos, Comput, Environ. Urban Syst. 54 (2015) 240–254, https://doi.org/10.1016/j.compenvurbsys.2015.09.001.
[62] T. Luo, X. Zheng, G. Xu, K. Fu, W. Ren, An improved DBSCAN algorithm to detect stops in individual trajectories, ISPRS Int. J. Geo-Inf. 6 (2017) 1–16, https://doi.org/10.3390/ijgi6030063.
[63] A. Cuttone, S. Lehmann, M.C. González, Understanding predictability and exploration in human mobility, EPJ Data Sci 7 (2018) 2, https://doi.org/10.1140/epjds/s13688-017-0129-1.
[64] P. Mazumdar, B.K. Patra, R. Lock, S.B. Korra, An approach to compute user similarity for GPS applications, Knowl. Base Syst. 113 (2016) 125–142, https://doi.org/10.1016/j.knosys.2016.09.017.
[65] Y. Yuan, M. Raubal, Y. Liu, Correlating mobile phone usage and travel behavior - a case study of Harbin, China, Comput, Environ. Urban Syst. 36 (2012) 118–130, https://doi.org/10.1016/j.compenvurbsys.2011.07.003.
[66] S. Datla, S. Sharma, Impact of cold and snow on temporal and spatial variations of highway traffic volumes, J. Transport Geogr. 16 (2008) 358–372, https://doi.org/10.1016/j.jtrangeo.2007.12.003.
[67] D.A. Call, The effect of snow on traffic counts in western New York state, Weather. Clim. Soc. 3 (2011) 71–75, https://doi.org/10.1175/WCAS-D-10-05008.1.
[68] T.H. Maze, M. Agarwal, G. Burchett, Whether weather matters to traffic demand, traffic safety, and traffic operations and flow, Transp. Res. Rec. J. Transp. Res. Board. 1948 (2006) 170–176, https://doi.org/10.1177/0361198106194800119.
[69] X. Lu, E. Wetter, N. Bharti, A.J. Tatem, L. Bengtsson, Approaching the limit of predictability in human mobility, Sci. Rep. 3 (2013) 1–9, https://doi.org/10.1038/srep02923.
[70] M.C. da M. Martins, A.N. Rodrigues da Silva, N. Pinto, An indicator-based methodology for assessing resilience in urban mobility, Transport. Res. Transport Environ. 77 (2019) 352–363, https://doi.org/10.1016/j.trd.2019.01.004.

[71] S. Datla, S. Sharma, Impact of cold and snow on temporal and spatial variations of highway traffic volumes, J. Transport Geogr. 16 (2008) 358–372, https://doi.org/10.1016/j.jtrangeo.2007.12.003.
[72] X. Liu, S. Yang, T. Ye, R. An, C. Chen, A new approach to estimating flood-affected populations by combining mobility patterns with multi-source data: a case study of Wuhan, China, Int. J. Disaster Risk Reduc. 55 (2021) 102106, https://doi.org/10.1016/j.ijdrr.2021.102106.
[73] Z. Cong, Z. Chen, D. Liang, Barriers to preparing for disasters: age differences and caregiving responsibilities, Int. J. Disaster Risk Reduc. 61 (2021) 102338, https://doi.org/10.1016/j.ijdrr.2021.102338.
[74] L. Yang, Y. Wang, Q. Bai, S. Han, Urban form and travel patterns by commuters: comparative case study of wuhan and xi'an, China, J. Urban Plann. Dev. 144 (2018), 05017014, https://doi.org/10.1061/(ASCE)UP.1943-5444.0000417.